Available online at www.elixirpublishers.com (Elixir International Journal)

Applied Chemistry

Elixir Appl. Chem. 81 (2015) 32030-32035

ISSN: 2229-712X

Activated Charcoal Supported Cadmium Doped TIO_2 for Photocatalytic and Antibacterial Applications

S.Prabha, V. L. Chandraboss, J.Kamalakannan and S. Senthilvelan*

Department of Chemistry, Annamalai University, Annamalai Nagar 608002, India.

ARTICLE INFO

Article history:

Received: 15 November 2014;

Received in revised form:

19 April 2015;

Accepted: 28 April 2015;

Keywords

Nanocomposites,

Photocatalytic,

Raman Spectroscopy,

X-Ray diffraction,

Antibacterial activity.

ABSTRACT

The photocatalytic activity was studied under UV light using AC-Cd/TiO_2 prepared via precipitation method and characterized by powder X-ray diffraction (XRD) , high resolution scanning electron micrographs (HR-SEM) with energy dispersive X-ray analysis (EDX), photoluminescence (PL) and Fourier transform Raman analysis (FT-RAMAN). The enhanced photo catalytic activity of the AC-Cd/TiO_2 is demonstrated through photodegradation of methylene blue under UV light radiation at 365 nm. The mechanism of photocatalytic effect of AC-Cd/TiO_2 Nano composite material has been discussed Further its antibacterial activity against two gram positive and two gram negative bacterial strain is studied.

Introduction

Textile industries produce extensive volume of coloured effluents. Among the different types of dyes used in industries, 65-75% belongs to azo compounds. The release of these coloured dyes in the ecosystem without treatment creates extreme environmental pollution problem by releasing toxic and potential carcinogenic substances into the aqueous phase and damaging to the aesthetic nature of the environment [1]. Many traditional techniques such as precipitation, adsorption, air stripping, reverse osmosis, ultra filtration and coagulation have been utilized so far the waste water treatment but they lost their vitality due to usually non destructive nature towards target molecules and they generate auxiliary pollutants of transferring contaminants from water to another phase[2]

Hence it is important to develop treatment methods that are more viable in destructing dyes from waste water. The removal of azo-dyes by advanced oxidation processes (AOPs) has been the subject of several recent studies. The mechanism of dye destruction in AOPs is based on the formation of a extremely reactive hydroxyl radical (•OH), that, with an oxidation potential of 2.80V can oxidize a broad range of organic compounds [3]. Photocatalysis, as a ‘‘green’’ technique, offers incredible potential in ecological remediation such as the photodegradation of the organic pollutants in the wastewater Semiconductor photocatalysts such as TiO_2 and ZnO nano particles have pulled much attention in recent years due to their various applications to the photocatalytic degradation of organic pollutants in water and air and dye sensitized photovoltaic solar cell.[4]

The interest is much more focused nowadays on the synthesis of photocatalyst materials to beat some limitations of the use of TiO_2. Some of the important limitations are: TiO_2 powder is hard to reuse, easy to agglomerate, and causes a issue of separation from the solution[5]. Many efforts have been paid to enhance the photocatalytic activity of semiconductor TiO_2 , such as semiconductor combination transition metal doping and noble metal deposition. Among these techniques doping with transition metals has been proved as an effective strategies to enhance photo catalyticactivity[1].

In industrial wastewaters brought about in the textile industry, the heavy metals (cations or complexes), even in traces will adsorb on the photocatalyst surface. Cadmium is one of the presumable heavy metals in these wastewaters. It can be adsorbed on the active sites in processes of chemisorption or it can be integrated in the TiO_2 latticeacting as a doping agent and immobilizing TiO_2 on an innert and suitable supporting materials. For this reason several porous media used as far as possible, to provide a tremendous pore structure for dispersing TiO_2 photocatalyst such as zeolite, alumina, silica, glass, carbon nano tube and activated charcoal.[6-10]

Among these materials, activated charcoal is widly utilized as a support it gas and water remediation due to its good adsorption properties and seems to be an attractive support for TiO_2.The increment in photocatalytic activity by the addition of charcoal has been well established.

In this work, we report the preparation, characterization, photocatalytic and antibacterial activity of AC-supported Cd doped TiO_2 nano composite materials. The obtained material was characterized by HR-SEM, with EDX, XRD, FT-RAMAN and PL Analysis. In the application part, we have studied their photocatalytic activity towards methylene blue in aqueous solution under UV light irradiation. The reason for choosing methylene blue is due to its wider applications that include colouring paper, temporary hair colourant, dyeing cottons, wools and coating for paper stock and thus acute exposure to MB will cause health problems such as increased heart rate, vomiting, shock, Heinz body formation, cyanosis and tissue neurosis in humans.[11]. AC-Cd/TiO_2 reveals enhanced photocatalytic activity as compared to TiO_2 and Cd/TiO_2 for the degradation of MB under UV light irradiation for 0-60 minutes. The enhanced photocatalytic activity of AC supported Cd/TiO_2 Iis caused by the reduction of the recombination of electron hole pairs, the extention of the light adsorption range increase of absorption of

Tele:

E-mail addresses: senthilvelanau@gmail.com

light intensity and enhancement of surface active sites. In addition, we report antibacterial activity of prepared AC-Cd/TiO_2 nano composite materials using three gram positive and two gram negative bacterias strains and ciprofloxacin used as a standard.the results shown AC-Cd/TiO_2 have higher bacterial activity than bare TiO_2 and cd dopped TiO_2 nano material.

Experimental section

Chemicals

Cadmium acetate dihydrate, titanium tetra isopropyl orthotitanate, activated charcoal, hydrochloric acid, ethanol and methylene blue were the guaranteed reagents of sigma Aldrich and used as such. Deionized water was used for all the reactions and treatment processes. All glassware's were cleaned with chromic acid followed by thoroughly washing with distilled water . Chemical structure of methylene blue is shown in Fig : 1

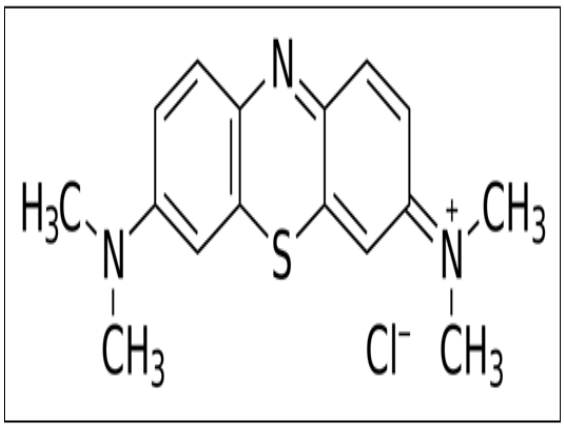

Figure 1. Chemical structure of Methylene Blue

Synthesis of Ac-Supported CD- Doped TIO_2 Nano Composite Materials

AC-Supported Cd doped TiO_2 nonocomposite material was synthesized by precipitation method. Inially cadmium acetate dihydrate (0.2 M) and Activated charcoal were dissolved in anhydrous ethanol (solution A). 2 ml of titanium tetraisopropyl ortho titanate (TTIP) is dissolved in ethanol is taken as another solution B. the solution B is added to Solution A and stirred well. To this 2-3 drops of conc.HNO_3 and 4 ml of conductivity water was added at room temperature under vigorous stirring until the precipitate formed.the obtained precipitate was washed with water and ethanol. Then the precipitate was collected and dried in oven at 100^oC for 12 hrs. The resulting powder was finally calcinated at 300^oC at 2 hrs.

Photocatalytic Activity

The photocatalytic activity of the prepared photocatalysts was evaluated by the photodegradation of MB by using multilamp photoreactor. The light source was a UV lamp (365nm). The reaction was maintained at ambient temperature (303 K). In a typical experiment, aqueous suspensions of dye (45 mL, 1 $\times 10^{-4}$ mol L^{-1}) and 0.06 g of the photocatalyst was loaded were in the reaction tube. Prior to irradiation, the suspension was magnetically stirred in the dark to ensure the establishment of an adsorption/desorption equilibrium. The suspension was kept under constant air-equilibrated condition. At the intervals of given irradiation time. The reaction solution was measured spectro photometrically (660 nm) by diluting it five times to keep the absorptions within the Beer–Lambert law limit.

Antibacterial Activity Study

Antibacterial activities of the synthesized TiO_2, Cd/TiO_2 and AC-Cd/TiO_2 nanoparticles were determined in comparison with Ciprofloxacin, using the disc diffusion assay method[12-14], is a means of measuring the effect of an anti microbialagent against bacteria grown in culture. The bacteria in question are swabbed uniformly across a culture plate. A filter-paper disk, impregnated with the compound to be tested, is then placed on the surface of the agar. The compound diffuses from the filter paper into the agar. The concentration of the compound will be highest next to the disk, and will decrease as distance from the disk increases. If the compound is effective against bacteria at a certain concentration, no colonies will grow where the concentration in the agar is greater than or equal to the effective concentration. This is the zone of inhibition. Thus, the size of the zone of inhibition is a measure of the compound's effectiveness: the larger the clear area around the filter disk, the more effective the compound. Approximately (20 mL) of molten and cooled media (Nutrient agar) was poured in sterilized Petri dishes.

The plates were left overnight at room temperature to check for any contamination to appear. The bacterial test organisms were grown in nutrient broth for 24 h. A (100 mL) nutrient broth culture of each bacterial organism (1×108 cfu/mL) was used to prepare bacterial lawns (cfu=number of colony forming unite). Antibiotic disks of 5 mm in diameter were impregnated with TiO_2, Cd/TiO_2 and AC-Cd/TiO_2 nanoparticles solution (60μg/ml).The plates were incubated at 37ºC and were examined for evidence of zones ofinhibition, which appeared as a clear area around the wells. The diameter of such zones of inhibition was measured using a meter ruler and the mean value for each organism was recorded and expressed in millimeter.

Analytical Methods

High resolution Scanning Electron Microscopy (HRSEM) and Elementary Dispersive X-ray (EDX) analysis experiments were carried out on a FEI Quanta FEG 200 instrument with EDX analyzer facility at 25 8C. XRD spectra was recorded on the X'PERT PRO model X-ray diffractometer from Pan Analytical instruments operated at a voltage of 40 kV and a current of 30 mA with Cu Ka radiation.

FT-RAMAN spectra were recorded with an integral microscope Raman system RFS27 spectrometer equipped with 1024 - 256 pixels liquefied nitrogen-cooled germanium detector. The 1064 nm line of the Nd:YAG laser (red laser) was used to excite. To avoid intensive heating of the sample, the laser power at the sample was not higher than 15 mW.

Each spectrum was recorded with an acquisition time of 18 s. UV–vis (ultraviolet and visible light) absorbance spectra were measured over a range of 200–800 nm with a Shimadzu UV-1650PC recording spectrometer using a quartz cell with 10 mm of optical path length. Photoluminescence spectra at room temperature were recorded using a perkin-Elmer LS 55 fluorescence spectrometer. Nano particles were dispersed in chloroform and excited using light of wavelength 300nm.

Results and discussion

Hr - Sem micrograph analysis

Figure (2a), (2b) and (2c) shows the HR-SEM images of the as prepared TiO_2, Cd/TiO_2 and AC-Cd/TiO_2.The surface morphology of TiO_2, Cd/TiO_2 and AC-Cd/TiO_2 has been studied using High Resolution Scanning Electron Microscope. The synthesized TiO_2 consisted of aggregated nanocrystalline anatase.

Due to its very small in size of anatase, nanoscale each particle had high driving force to agglomerate, thus the morphology shown by HR-SEM was secondary particles of agglomerated nano sized anatase. The Cd/TiO_2 particles exhibited irregular morphology due to the agglomeration of primary particles and with an average diameter of ~90 nm and AC-Cd/TiO_2 particles exhibited average diameter of ~85 nm.

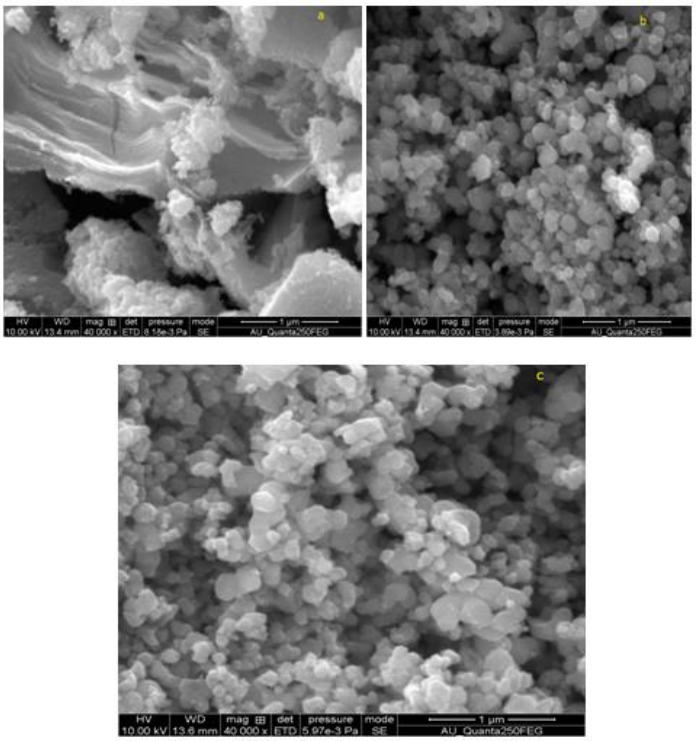

Figure 2. HR-SEM images of (a) TiO_2 (b) CD/TiO_2 (c) AC-CD/TiO_2

The observation particle size of the Cd/TiO_2 was greater than that of AC-Cd/TiO_2 reveals that absence of AC and also AC matrix controlled the growth of Cd/TiO_2 particles and prevents their agglomeration. Moreover, the decrease in the particle size can be correlated with the observed increase of the surface area[15]. Figure 3(a), 3(b) and 3(c) shows the EDX images of the as prepared TiO_2, Cd/TiO_2 and AC-Cd/TiO_2.

EDX analysis confirms only Titanium, cadmium and oxygen present Cd/TiO_2 (Figure 3b), where as Titanium, cadmium, oxygen and carbon present in AC-Cd/TiO_2 composite material (Figure 3c). EDX analysis of the composite sample confirms a doping of the Cd and C in the TiO_2 material.

XRD Patterns

The obtained XRD of the TiO_2, Cd/TiO_2 and AC-Cd/TiO_2 nanoparticle are shown in Fig. 4a , 4b and 4c. The TiO_2 peaks at 25.4, 37.5, 47.8, 54.7 and 62.4 , are the diffractions of the TiO_2 (1 0 1), (0 0 4), (2 0 0), (1 0 5) and (2 0 4) crystal planes. The experimental XRD pattern agrees with the JCPDS card no. 21-1272 (anatase TiO_2) and the XRD pattern of TiO_2 nanoparticles other literature [16]. The 2θ at peak 25.4° confirms the TiO_2 anatase structure [17]. Cd/TiO_2 peaks at 25.4, 34.2, 37.7, 47.8, 54.5, 62.8, and 69.1 are the diffractions of the TiO2 (101), Cd (111), (JC PDS File No. 05-0640) TiO2 (004), TiO2 (200), TiO2 (105), TiO2 (204), Cd(222).

AC-Cd/TiO_2 peaks at 13, 25.4, 29.3, 33.4, 37.7, 47.8, 54.5, 62.8, and 70.6 are the diffractions of the C (002), TiO2 (101), C(002), Cd (111), (JC PDS File No. 05-0640) TiO_2 (004), TiO_2 (200), TiO_2 (105), TiO_2 (204), Cd(222). Two peaks with a value of 2θ around 13, 29.3 (JCPDS card no.50 0927) are assigned as graphite oxide and graphite carbon.

The average crystalline size (L) of the TiO_2 and AC-Cd/TiO_2 particles can be calculated from the Debye–Scherrer formula [15], $L = 0.89l/b \cos \theta$ where L is the crystalline size (in nm), l is the wavelength (in nm), b is the full width at half maximum intensity (FWHM-in radian), and θ is the Bragg diffraction angle.

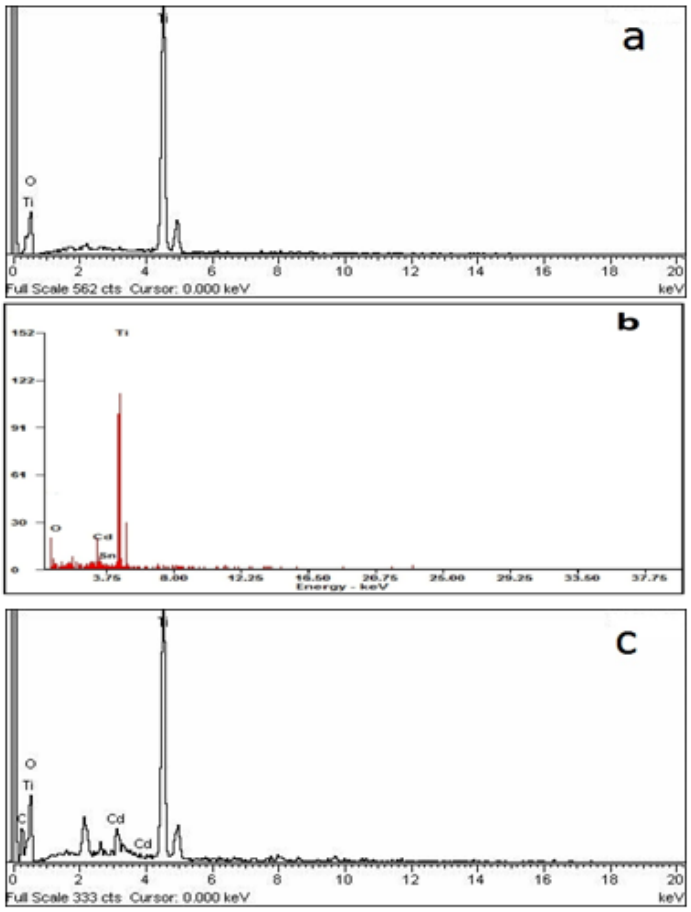

Figure 3a. EDX Spectrum of TiO_2 (b) Cd/TiO_2 (c) AC-Cd/TiO_2

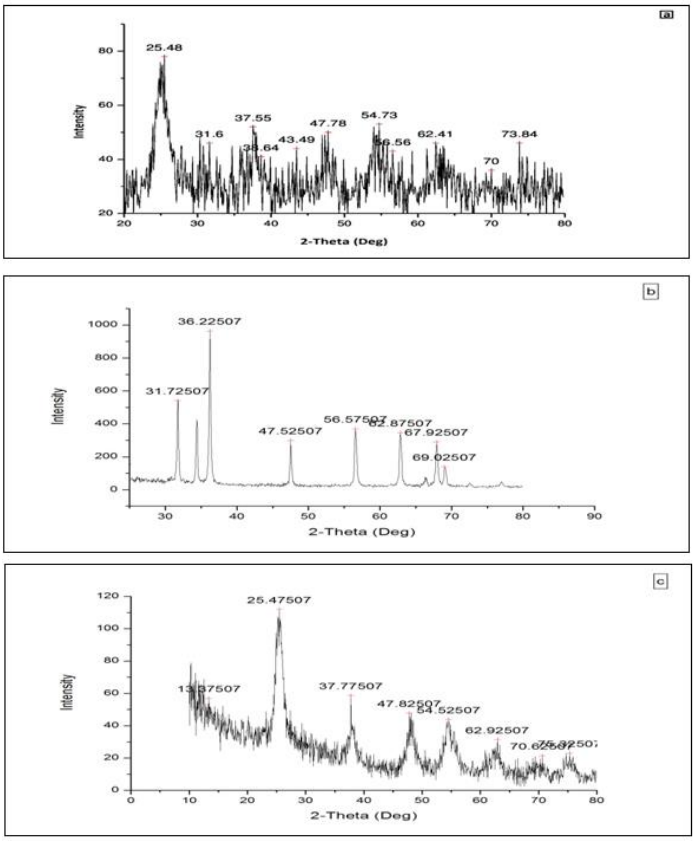

Figure 4. XRD patterns of (a)TiO_2 Nano material, (b) CD/TiO_2 Nanocomposite materials and (c) AC-Cd/TiO_2 Nanocomposite material

The average crystalline size of Cd/TiO_2 product was figured out to be about 88 nm. The average crystalline size of AC-Cd/TiO_2 particles are almost 82 nm. As can be understood, these values are very close to the SEM value.

Ft-Raman Analysis

Fig. 5a & 5b presents the Raman spectrum of the Cd/TiO_2 and AC-Cd/TiO_2. The Raman peaks observed at 197.1, 398.4, 518.7 and 644.0 cm^{-1} in Fig. 5 are assigned as the Eg, B1g, A1g + B1g, and Eg modes[18] of Cd/TiO_2 . AC-Supported Cd/TiO_2 consists of of peaks at 151.1,

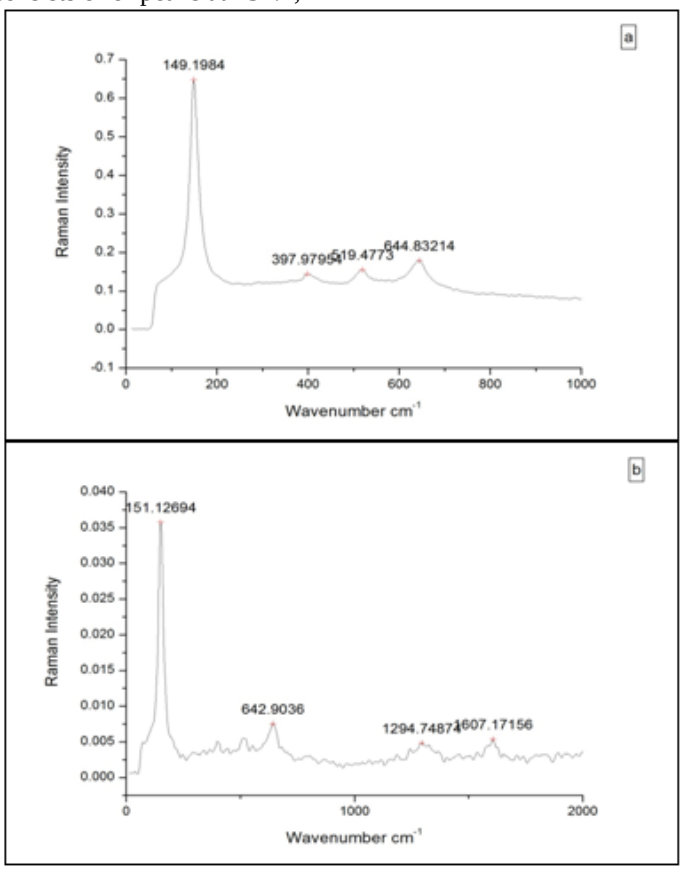

Figure 5, FT-RAMAN Spectra of (a) CD/TiO_2 Nanocomposites and (b) AC-CD/TiO_2 Nano composite material

399.67, 642.28, 511.5 and 1606. The high intensity of the 1325cm^{-1} and 1606 cm^{-1}, attributed to the D- and G-bands of Carbon, respectively. Which correspond to carbon present in the Cd/TiO_2 material[19]

Pl Analysis

Photoluminescence spectra of TiO_2, Cd/TiO_2 and AC-Cd/TiO_2 $_{are}$ shown in figure 6a,6b and 6c respectively. As the photoluminescence occurs due to electron hole recombination, its intensity is directly proportional to the rate of electron-hole recombination. TiO_2 gave emissions at 362, 378, 390, 410, 438, 460, 491 The Photoluminescence spectrum of anatase phase nano TiO_2 resulted from three origins: self trapped excitons [20,21] surface states [22] and oxygen vacancies. The peak situated at 431 nm corresponds to the emission band of self-trapped excitons of the TiO_2 nanoparticles. As it has been reported by Liu et al. [23], a strong emission at 491 nm could be attributed to the indirect recombination via defect states with the interaction of phonons in TiO_2 lattice Oxygen vacancy peaks normally observed at 391nm and 409 nm. the peak with the center at 371 nm could be attributed to the intrinsic emission of the TiO_2. The PL Spectrum of Cd/TiO_2 nanoComposites show as in the case of undoped TiO_2 and there is no significant shift in the position of the undoped TiO_2 on Cd substitution. AC-Cd/TiO2 gave five emissions at 362, 376, 410, 436 and 490 nm. Cd doping TiO2 and AC Supported Cd/TiO_2 slightly shift the emission of Undoped TiO_2. The intensity of AC-Cd/TiO_2 . PL emission is less when compared to TiO_2 and Cd/TiO_2 nano composite materials. A weaker PL emission signal is commonly indicative of higher photocatalytic activity[24,25]. The AC-Cd/TiO_2 presented very low emission intensities, indicating that the residual carbon species significantly reduced the recombination rate of the photo-induced electrons and holes[26]

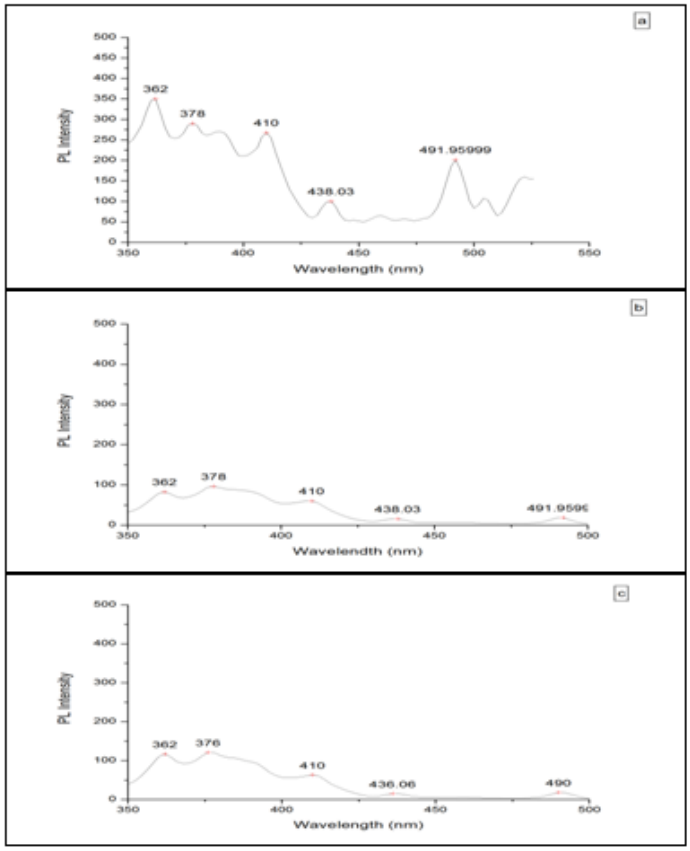

Figure 6. PL Spectra of (a) TiO2 Nanomaterial (b) CD/TiO_2 Nano composite material and (c) AC-CD/TiO_2 Nanocomposite material

Photodegradation and Decolourization of Mb Under UV Light Irradiation

The textile industries daily discharge million litres of untreated effluents in the form of wastewater into public drains that eventually empty into rivers. This alters the pH, increases the biochemical oxygen demand, chemical oxygen demand (COD) and gives the rivers intense colouration. The use of these water resources is limited and the ecosystem is affected. The removal of the polluting dyes is an important problem[27]. So We have chosen photodegradation of MB as model dye with UV irradiation to evaluate the photocatalytic activity of the proposed photocatalyst. Fig. 6 shows the time course of decrease in the concentration of MB under UV irradiation. The photodegradation process of MB, the UV-vis spectra and the colours of MB aqueous solution as a function of under UV light irradiation time in the presence of photocatalysts(TiO_2**,** Cd/TiO_2 and AC-Cd/TiO_2) are illustrated in Figures 7a , 7b, and 7c.It can be seen from UV-visible spectra changes , while in the case of MB two peaks were initially observed at 663 and 612nm, which merged and the maximum absorbance was finally observed at around 636nm, the strong adsorption peak of MB solution at 636 nm steadily decreased and degraded with increasing the light irradiation time, and the initial blue colour of the solution gradually turned to light – coloured. The comparative study of

photocatalytic activity of TiO_2, Cd/TiO_2 and $AC\text{-}Cd/TiO_2$ photocatalysts for photodegradation of MB was shown in figure 7d. $AC\text{-}Cd/TiO_2$ exhibited excellent photocatalytic activity for MB under UV light irradiation when compared to that of TiO_2 & Cd/TiO_2 .

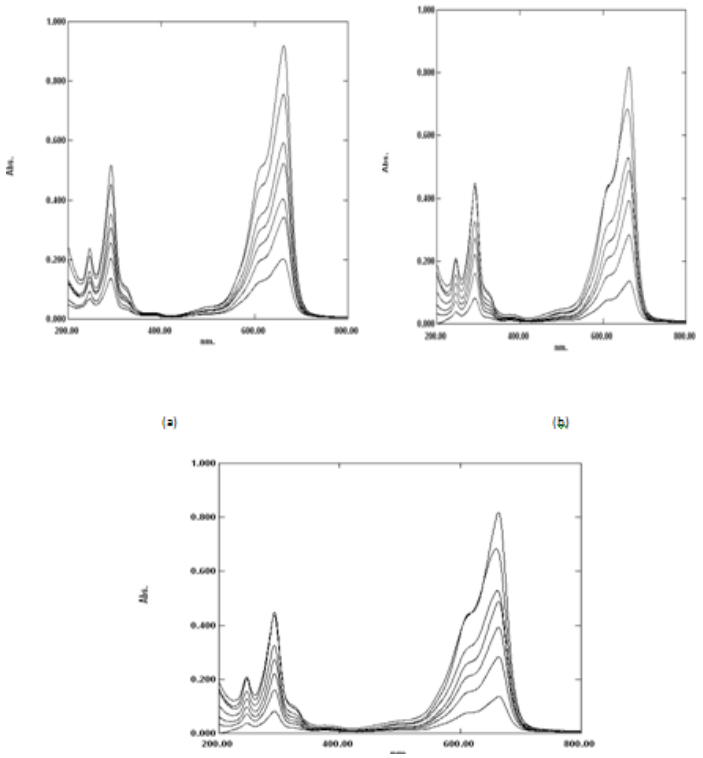

Figure 7. Absorption spectral changes of Methylene blue solution (1×10^{-4} M, 45 ml) in the presence of Photocatalyst (a) TiO2 (b) CD/TiO_2 (c) $AC\text{-}CD/TiO_2$ under UV light irradiation at 10 min interval.

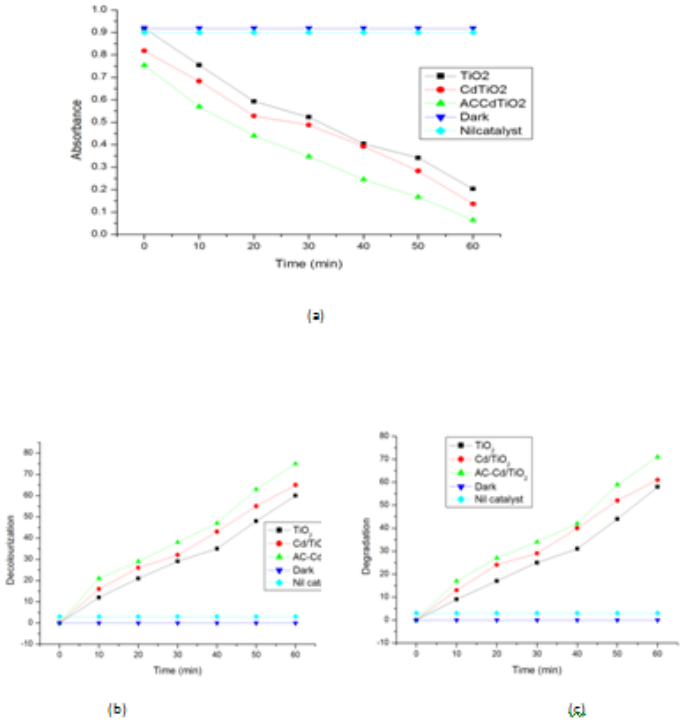

Figure 8a. Comparative studies of Photocatalytic activity (Absorbance Vs time (min) of (a) TiO2 (b) CD/TiO_2 (c) $AC\text{-}CD/TiO_2$

Photocatalyst for photodegradation and decolourization of MB under UV light irradiation at 10 minute interval. (b) Comparison of photocatalytic activity(dye decolourization (%) Vs time (min) of decolourization of MB dye by (a) TiO_2 (b) Cd/TiO_2 (c) $AC\text{-}Cd/TiO_2$ under UV light irradiation at 10 min interval. (c) comparative studies of photocatalytic activity (degradation (%) Vs time (min) of degradation of MB dye by (a) TiO2 (b) Cd/TiO_2 (c) $AC\text{-}Cd/TiO_2$ under UV light irradiation at 10 minute interval.

The effect of time on the degradation of MB was examined under UV light irradiation in the reaction time ranging from 0 to 60 minutes. Samples were withdrawn at different time intervals after photodegradation and centrifuged immediately and percentage mineralisation was studied.

Results show that as time increases the percentage decolourization increases. It has been observed that the decolourization of the compound proceeds much more rapidly in the presence of $AC\text{-}Cd/TiO_2$ doped catalyst in UV light. The reason for better photoactivity could be attributed to the fact that the catalyst is composed of nanocrystalline form. The presence of dopant prevents the recombination of photogenerated electrons and holes leading to better photocatalytic activity.

Mechanism

Based on previous reports, the photocatalytic degradation of MB under UV or visible light irradiation is mainly related to the generation of reactive hydroxy and hydroperoxy radicals [28–30]. The hydroxy and hydroperoxy radicals produced by the action of photocatalyst are capable of oxidizing MB molecules at the surface layer of photocatalyst. MB molecules tend to be adsorbed by the surface of the catalyst[31].

In water, UV-irradiated $Cd\text{-}TiO_2$ is able to completely destroy organic contaminants through the TiO_2 activation, according to the following reaction.

$AC\text{-}Cd/TiO_2 + h\gamma\ (UV) \longrightarrow AC\text{-}Cd/TiO_2\ (e^-_{CB} + h^+_{VB})$

$AC\text{-}Cd/TiO_2\ (h^+_{VB}) + H2O \longrightarrow AC\text{-}Cd/TiO_2 + H+ + OH\cdot$

$AC\text{-}Cd/TiO_2\ (h^+_{VB}) + OH- \longrightarrow AC\text{-}Cd/TiO_2 + OH\cdot$

$AC\text{-}Cd/TiO_2\ (e^-_{CB}) + O_2 \longrightarrow AC\text{-}Cd/TiO_2 + O_2\cdot-$

$O_2\cdot- + H+ \longrightarrow HO\cdot_2$

The electron and the hole are generated in the conduction band and in the valence band of TiO_2 by UV irradiation, respectively [32]. The positive hole can oxidize hydroxide ions (or water molecule) adsorbed on the surface of TiO_2 particles to produce hydroxyl radical [33], the electrons of conduction band can react with the oxygen to produce superoxide radical anions [34]. The superoxide radical anion reacts with a proton to form hydroperoxyl radical.

The hydroxyl radical existing on the surface of catalyt accelerated the degradation of MB.

$MB* + AC\text{-}Cd/TiO_2 \longrightarrow MB\cdot+e_{CB}\ (AC\text{-}Cd/TiO_2)$

$O_2 + e- \longrightarrow O_2\cdot-$

$MB\cdot+ + OH- \longrightarrow MB + OH\cdot$

$MB\cdot+ + OH\cdot \longrightarrow products$

$MB\cdot+ + O_2\cdot- \longrightarrow products$

For the mechanism of photosensitized oxidation, in the presence of catalysts the excited state of MB injects an electron into the conduction band. The MB dye is then converted to a cationic dye radical that undergoes degradation to yield products.

Antibacterial Activity

Antibacterial activity of TiO_2, Cd/TiO_2 and $AC\text{-}Cd/TiO_2$ nano composite materials are shown in Table 1. The antimicrobial properties of TiO_2, Cd/TiO_2 and $AC\text{-}Cd/TiO_2$ nano composite materials were studied against Gram positive bacteria

namely Bacillus subtilus, Staphylococcus aureus and Gram negative bacteria Escherichia coli, Pseudomonas aeruginosa with a size dependent effect.

Table 1. Antibacterial activity [disc diffusion method]

S. No.	Bacteria	Standard Antibiotic Disk*	Zone of inhibition (mm)			
			TiO_2	Cd/TiO_2	AC-Cd/TiO2	Control (DMSO)
1	Bacillus subtilis	22	14	16	17	-
2	Escherichia coli	24	10	13	16	-
3	Pseudomonasaeruginosa	24	09	14	14	-
4	Staphylococcus aureus	22	11	13	16	-

*ciprofloxacin

17 mm zone of inhibition was developed against B. subtilis which was the biggest zone developed against this strain by AC-Cd/TiO_2 nano composite materials but it show 16 mm against the other gram-positive strain Staphylococcus aureus**.** The improved activity was because of its small size compared with TiO_2 and Cd/TiO_2

AC-Cd/TiO_2 nano composite materials showed activity against both gram-positive strains and also gram-negative strains. 16mm and 14mm inhibition zone was developed against Escherichia coli and Pseudomonas aeruginosa. AC-Cd/TiO_2 nano composite materials were found good against gram-positive bacteria rather than gram-negative. This was due to the differences in the cell wall composition of these two bacteria.

Conclusion

AC Supported cadmium doped TiO_2 nanocomposite material was prepared by a precipitation method .This material was characterized by powder X-ray diffraction (XRD) , high resolution scanning electron micrographs(HRSEM) with energy dispersive X-ray analysis, photoluminescence (PL) and Fourier transform Raman analysis(FT-RAMAN).These results confirmed the formation of AC-Cd/TiO_2 nanocomposite material.HR SEM and XRD analysis of Cd/TiO_2 showed the average size of as 90nm, AC-Cd/TiO_2 showed the average particle size of as 85nm.moreover the decrease in particle size can be correlated with increase of the surface area .The EDX shows the presence of C and Cd in the TiO_2 material.XRD reveal the all strong peaks can be indexed as anatase form of TiO_2. PL Spectra explain the suppression of recombination of the photogenerated electron hole pairs by AC-Cd/TiO_2 nano material. AC-Cd/TiO_2 reveals enhanced photocatalytic activities as compared to TiO_2 and Cd/TiO_2 for the photodegradation and decolourization of MB under UV light irradiation for 0 to 60 minutes. The mechanism of photo catalytic effect of AC-Cd/TiO_2 nano composite material has been discussed.

Reference

1. Dongfang Zhang et al., J Mater Sci, 47 (2012) 2155-2161
2. Adel A Ismail et al., chemical Engineering Journal., 229 (2013), 225-233
3. Nadia Riaz et al., chemical Engineering Journal., 185-186(2012) 108-119
4. Senthilvelan S et al., Material Research Bulletin , 48(2013) 3707-3712
5. Housda Slimen et al., Journal of photochemistry and photobiology, 221(2011) 13-21
6. M V Shankar et al., chemosphere , 63(2006) 1014-1021
7. X Zhang et al., Applied catalysis A: General, 282(2005) 285-293
8. T Yazawa et al., Ceramics International , 35(2009) 3321-3325
9. Y Yu et al., Applied catalysis General, 289(2005), 186-196
10. B Thyba., Applied catalysis B: Environmental, 41(2003) 427-433.
11. Karakitsou K Eet al., J Phys.Chem, 97(1993) 1184.
12. 1. In: Microbiological assays and tests, Indian Pharmacopoeia, Ministry of Health and Family Welfare, The Controller of Publications, New Delhi, A-100 (1996).
13. 2. H.W. Seely and P. J. Van Demark., A Laboratory Manual of Microbiology, Taraporewala Sons and Co., Mumbai, 55 (1975).
14. 3. A. L. Barry., The antimicrobial susceptibility test. Principle and Practice, Lea and Febiger, Philadelphia, 180 (1976).
15. Mohd Athar., Adv. Mater. Rev. 1(1)(2014) 25-37
16. Antic Z, Krsmanovic RM, Nikolic MG, Cincovic MM, Mitric M, Polizzi S, Dramicanin MD., Multisite luminescence of rare earth doped TiO2 anatase nanoparticles. Mat.Chem.Phys. 135(2012) 1064-1069.
17. Ba-Abbad M, Kadhum AH, Mohamad A, Takriff MS, Sopian K, Synthesis and Catalytic Activity of TiO_2 Nanoparticles for Photochemical Oxidation of Concentrated Chlorophenols under Direct Solar Radiation Int.J.Electrochem.Sci. 7(2012) 4871-4888.
18 Ohsaka, T. J. Phys. Soc. Jpn. 48(**1980)** 1661.
19 B. W. Mwakikunga., Nanoscale Res Lett 3 (2008) 421–426
20 L.V. Saraf, S.I. Patil, S.B. Ogalae, S.R. Sainkar, S.T. Kshirsager, Int. J. Mod. Phys. B12 (1998) 2635.
21 H. Tang, H. Berger, P.E. Schmid, F. Levy, Solid State Commun. 87 (1993) 847.
22 L. Fross, M. Schubnell, Appl. Phys. B: Photophys. Laser chem. 56 (1993) 363.
23 Liu B., Zhao X., Zhao Q., He X., Feng., J Journal of Electron Spectroscopy and Related Phenomena **148**(3)(2005) 158–63.
24 Chen, X.F., Wang, X.C., Hou, Y.D., Huang, J.H., Wu, L., Fu, X.Z., J. Catal. 255(1)(2008) 59–67.
25 He, Z.L., Zhu, Z.F., Li, J.Q., Zhou, J.Q., Wei, N., J. Hazard. Mater. 190(1-3)(2011) 133–139.
26 Yu, J.G., Ma, T.T., Liu, S.W.,Phys. Chem. Chem. Phys. 13(8)(2011) 3491– 3501.
27 Darshan Marjadi., International Journal of Chemtech Applications 2(2)(2003) 126-136.
28 Tschirch, J.; Dillert, R.; Bahnemann, D.; Proft, B.; Biedermann, A.; Goer, B. Res. Chem. Intermed. 34(**2008)** 381–392.
29 45. Fu, P.-F.; Zhao, Z.; Peng, P.; Dai, X.-G. Chin. J. Process Eng. 8(**2008)** 65–71.
30 46. Kim, J.; Choi, W.; Park, H. Res. Chem. Intermed. 36(**2010)** 127–140.
31 Tursun Abdiryim et al., Materials 7(2014) 3786-3801
32 H. A. Le, L. T. Linh, S. Chin, and J. Jurng, Powder Technology, 225(2012) 167–175,
33 R.-J. Wu, C.-C. Chen, C.-S. Lu, P.-Y. Hsu, and M.-H. Chen, Desalination, 250(3)(2010) 869–875
34 G. Wang, F. Wu, X. Zhang, M. Luo, and N. Deng, Journal of Hazardous Materials, vol. 133(1-3)(2006) 85–91.